

# JES

JOURNAL OF  
ENVIRONMENTAL  
SCIENCES

April 1, 2015 Volume 30  
[www.jesc.ac.cn](http://www.jesc.ac.cn)

ISSN 1001-0742  
CN 11-2629/X



## MBR in Wastewater Reclamation



Sponsored by  
Research Center for Eco-Environmental Sciences  
Chinese Academy of Sciences

**Highlight articles**

- 129 Rice: Reducing arsenic content by controlling water irrigation  
Ashley M. Newbigging, Rebecca E. Paliwoda and X. Chris Le
- 132 Apportioning aldehydes: Quantifying industrial sources of carbonyls  
Sarah A. Styler

**Review articles**

- 30 Application of constructed wetlands for wastewater treatment in tropical and subtropical regions (2000-2013)  
Dong-Qing Zhang, K.B.S.N. Jinadasa, Richard M. Gersberg, Yu Liu, Soon Keat Tan and Wun Jern Ng
- 47 Stepwise multiple regression method of greenhouse gas emission modeling in the energy sector in Poland  
Alicja Kolasa-Wiecek
- 113 Mini-review on river eutrophication and bottom improvement techniques, with special emphasis on the Nakdong River  
Andinet Tekile, Ilho Kim and Jisung Kim

**Regular articles**

- 1 Effects of temperature and composite alumina on pyrolysis of sewage sludge  
Yu Sun, Baosheng Jin, Wei Wu, Wu Zuo, Ya Zhang, Yong Zhang and Yaji Huang
- 9 Numerical study of the effects of local atmospheric circulations on a pollution event over Beijing-Tianjin-Hebei, China  
Yucong Miao, Shuhua Liu, Yijia Zheng, Shu Wang and Bicheng Chen, Hui Zheng and Jingchuan Zhao
- 21 Removal kinetics of phosphorus from synthetic wastewater using basic oxygen furnace slag  
Chong Han, Zhen Wang, He Yang and Xiangxin Xue
- 55 Abatement of SO<sub>2</sub>-NO<sub>x</sub> binary gas mixtures using a ferruginous active absorbent: Part I. Synergistic effects and mechanism  
Yinghui Han, Xiaolei Li, Maohong Fan, Armistead G. Russell, Yi Zhao, Chunmei Cao, Ning Zhang and Genshan Jiang
- 65 Adsorption of benzene, cyclohexane and hexane on ordered mesoporous carbon  
Gang Wang, Baojuan Dou, Zhongshen Zhang, Junhui Wang, Haier Liu and Zhengping Hao
- 74 Flux characteristics of total dissolved iron and its species during extreme rainfall event in the midstream of the Heilongjiang River  
Jiunian Guan, Baixing Yan, Hui Zhu, Lixia Wang, Duian Lu and Long Cheng
- 81 Sodium fluoride induces apoptosis through reactive oxygen species-mediated endoplasmic reticulum stress pathway in Sertoli cells  
Yang Yang, Xinwei Lin, Hui Huang, Demin Feng, Yue Ba, Xuemin Cheng and Liuxin Cui
- 90 Roles of SO<sub>2</sub> oxidation in new particle formation events  
He Meng, Yujiao Zhu, Greg J. Evans, Cheol-Heon Jeong and Xiaohong Yao
- 102 Biological treatment of fish processing wastewater: A case study from Sfax City (Southeastern Tunisia)  
Meryem Jemli, Fatma Karray, Firas Feki, Slim Loukil, Najla Mhiri, Fathi Aloui and Sami Sayadi

## CONTENTS

- 122 Bioreduction of vanadium (V) in groundwater by autohydrogentrophic bacteria: Mechanisms and microorganisms  
Xiaoyin Xu, Siqing Xia, Lijie Zhou, Zhiqiang Zhang and Bruce E. Rittmann
- 135 Laccase-catalyzed bisphenol A oxidation in the presence of 10-propyl sulfonic acid phenoxazine  
Rūta Ivanec-Goranina, Juozas Kulys, Irina Bachmatova, Liucija Marcinkevičienė and Rolandas Meškys
- 140 Spatial heterogeneity of lake eutrophication caused by physiogeographic conditions: An analysis of 143 lakes in China  
Jingtao Ding, Jinling Cao, Qigong Xu, Beidou Xi, Jing Su, Rutai Gao, Shouliang Huo and Hongliang Liu
- 148 Anaerobic biodegradation of PAHs in mangrove sediment with amendment of  $\text{NaHCO}_3$   
Chun-Hua Li, Yuk-Shan Wong, Hong-Yuan Wang and Nora Fung-Yee Tam
- 157 Achieving nitrification at low temperatures using free ammonia inhibition on *Nitrobacter* and real-time control in an SBR treating landfill leachate  
Hongwei Sun, Yongzhen Peng, Shuying Wang and Juan Ma
- 164 Kinetics of Solvent Blue and Reactive Yellow removal using microwave radiation in combination with nanoscale zero-valent iron  
Yanpeng Mao, Zhenqian Xi, Wenlong Wang, Chunyuan Ma and Qinyan Yue
- 173 Environmental impacts of a large-scale incinerator with mixed MSW of high water content from a LCA perspective  
Ziyang Lou, Bernd Bilitewski, Nanwen Zhu, Xiaoli Chai, Bing Li and Youcai Zhao
- 180 Quantitative structure-biodegradability relationships for biokinetic parameter of polycyclic aromatic hydrocarbons  
Peng Xu, Wencheng Ma, Hongjun Han, Shengyong Jia and Baolin Hou
- 191 Chemical composition and physical properties of filter fly ashes from eight grate-fired biomass combustion plants  
Christof Lanzerstorfer
- 198 Assessment of the sources and transformations of nitrogen in a plain river network region using a stable isotope approach  
Jingtao Ding, Beidou Xi, Qigong Xu, Jing Su, Shouliang Huo, Hongliang Liu, Yijun Yu and Yanbo Zhang
- 207 The performance of a combined nitrification-anammox reactor treating anaerobic digestion supernatant under various C/N ratios  
Jian Zhao, Jiane Zuo, Jia Lin and Peng Li
- 215 Coagulation behavior and floc properties of compound bioflocculant-polyaluminum chloride dual-coagulants and polymeric aluminum in low temperature surface water treatment  
Xin Huang, Shenglei Sun, Baoyu Gao, Qinyan Yue, Yan Wang and Qian Li
- 223 Accumulation and elimination of iron oxide nanomaterials in zebrafish (*Danio rerio*) upon chronic aqueous exposure  
Yang Zhang, Lin Zhu, Ya Zhou and Jimiao Chen
- 231 Impact of industrial effluent on growth and yield of rice (*Oryza sativa* L.) in silty clay loam soil  
Mohammad Anwar Hossain, Golum Kibria Muhammad Mustafizur Rahman, Mohammad Mizanur Rahman, Abul Hossain Molla, Mohammad Mostafizur Rahman and Mohammad Khabir Uddin
- 241 Molecular characterization of microbial communities in bioaerosols of a coal mine by 454 pyrosequencing and real-time PCR  
Min Wei, Zhisheng Yu and Hongxun Zhang
- 252 Risk assessment of *Giardia* from a full scale MBR sewage treatment plant caused by membrane integrity failure  
Yu Zhang, Zhimin Chen, Wei An, Shumin Xiao, Hongying Yuan, Dongqing Zhang and Min Yang
- 186 Serious BTEX pollution in rural area of the North China Plain during winter season  
Kankan Liu, Chenglong Zhang, Ye Cheng, Chengtang Liu, Hongxing Zhang, Gen Zhang, Xu Sun and Yujing Mu

Available online at [www.sciencedirect.com](http://www.sciencedirect.com)

ScienceDirect

[www.journals.elsevier.com/journal-of-environmental-sciences](http://www.journals.elsevier.com/journal-of-environmental-sciences)

# Adsorption of benzene, cyclohexane and hexane on ordered mesoporous carbon

Gang Wang<sup>1</sup>, Baojuan Dou<sup>1</sup>, Zhongshen Zhang<sup>1</sup>, Junhui Wang<sup>1</sup>,  
Haier Liu<sup>2</sup>, Zhengping Hao<sup>1,\*</sup>

1. Research Center for Eco-Environmental Sciences, Chinese Academy of Sciences, Beijing 100085, China. E-mail: [wgbift@126.com](mailto:wgbift@126.com)

2. School of Materials Science and Engineering, University of Science and Technology Beijing, Beijing 100083, China

## ARTICLE INFO

### Article history:

Received 15 May 2014

Revised 6 October 2014

Accepted 10 October 2014

Available online 23 February 2015

### Keywords:

Volatile organic compounds

Adsorption

Ordered mesoporous carbon

Isosteric heat of adsorption

Knudsen diffusion

## ABSTRACT

Ordered mesoporous carbon (OMC) with high specific surface area and large pore volume was synthesized and tested for use as an adsorbent for volatile organic compound (VOC) disposal. Benzene, cyclohexane and hexane were selected as typical adsorbates due to their different molecular sizes and extensive utilization in industrial processes. In spite of their structural differences, high adsorption amounts were achieved for all three adsorbates, as the pore size of OMC is large enough for the access of these VOCs. In addition, the unusual bimodal-like pore size distribution gives the adsorbates a higher diffusion rate compared with conventional adsorbents such as activated carbon and carbon molecular sieve. Kinetic analysis suggests that the adsorption barriers mainly originated from the difficulty of VOC vapor molecules entering the pore channels of adsorbents. Therefore, its superior adsorption ability toward VOCs, together with a high diffusion rate, makes the ordered mesoporous carbon a promising potential adsorbent for VOC disposal.

© 2015 The Research Center for Eco-Environmental Sciences, Chinese Academy of Sciences.

Published by Elsevier B.V.

## Introduction

Volatile organic compounds (VOCs) are a class of air pollutants in industrial processes and daily human consumption (Lin et al., 2011; Parmar and Rao, 2009; He et al., 2012; Hernandez et al., 2003; Ghoshal and Manjare, 2002; Reguer et al., 2011; Gonzalez-Miquel et al., 2013). Because of their high vapor pressure and low boiling point, they are prone to be emitted into the atmosphere, causing great environmental problems because of their intrinsically hazardous properties. Not only they are the main precursors of photochemical reaction in the atmosphere, inducing ozone destruction and photochemical smog, but they are also toxic toward human health, and may cause pathogenic, mutagenic and even fatal diseases (Wang et al., 2007; Parmar and Rao, 2009;

He et al., 2012; Hernandez et al., 2003). Unfortunately, with the continuous development of industrialization in recent years, the emissions of VOCs have gradually increased to a new high level (Ghoshal and Manjare, 2002; Wu et al., 2011). In order to reduce the harmful effect of VOCs on the environment and humans, stringent regulations have already been enforced to limit further VOC emission. Meanwhile, the abatement technologies for VOCs have aroused great attention and they are considered a major component in the elimination of pollution.

Various kinds of methods, such as catalytic oxidation, adsorption, absorption, photocatalytic processes, and biological methods are employed for the abatement of VOCs (Wang et al., 2007; Parmar and Rao, 2009; He et al., 2012; Hernandez et al., 2003; Ghoshal and Manjare, 2002; Reguer et al., 2011;

\* Corresponding author. E-mail: [zpinghao@rcees.ac.cn](mailto:zpinghao@rcees.ac.cn) (Zhengping Hao).



Gonzalez-Miquel et al., 2013). Among them, adsorption technology seems to be the preferred choice due to its great advantages of convenience and high efficiency (Hernandez et al., 2003; Ghoshal and Manjare, 2002; Reguer et al., 2011). In addition, the adsorption process is an important intermediate step when considering the recovery of valuable VOCs (Ghoshal and Manjare, 2002; Ramirez et al., 2005). It is generally accepted that for adsorption technology, a proper adsorbent is important for the efficient removal of VOCs. Until now, activated carbon has been used as the most popular adsorbent due to its low cost and relatively good adsorption properties (Ramirez et al., 2005; Lillo-Rodenas et al., 2006; de Souza et al., 2012). However, some weaknesses have limited its further application. Activated carbon is a typical microporous adsorbent, with most pores in the micropore range (<2 nm), which may slow the transport velocity of VOC molecules. In addition, the irregularly shaped pores in activated carbon increase the diffusion resistance of adsorbate molecules during the adsorption process and a long time is needed to reach adsorption equilibrium (Nevskaia et al., 2004; Ji et al., 2010; Britt et al., 2008). Thus a new adsorbent with high specific surface area, large pore volume and relative larger pore size is urgently needed.

Ordered mesoporous carbon (OMC) is a kind of mesoporous material possessing high specific surface area, large pore volume and tunable pore size, which can be used as a catalyst support and adsorbent as well as in electric capacitors (Wang et al., 2013; Hartmann et al., 2005; Tanaka et al., 2013). Generally, OMC can be synthesized using low-molecular-weight resol as carbon source, silica as an additive and triblock copolymer Pluronic F127 as a structure-directing agent via the evaporation-induced self-assembly (EISA) method (Ma et al., 2013; Li and Zhao, 2013). Benefiting from its relatively large surface area and pore volume, OMC shows great potential advantages as an adsorbent in environmental remediation processes. Hartmann et al. (2005) investigated the adsorption properties of Vitamin E on mesoporous carbon molecular sieves, and the large adsorption amount indicated the superior adsorption properties of mesoporous carbon molecular sieves compared to microporous carbon adsorbents. In addition, they certified that the adsorption process takes place in the channels of the mesoporous carbon adsorbent, contrary to the conventional opinion that mesoporous channels only provide passage for adsorbate molecules rather than supplying efficient adsorption sites (Hartmann et al., 2005). Zhuang et al. (2009) used OMCs for the efficient disposal of wastewater containing bulky dye molecules for the first time. The results suggested that OMC can be used as an efficient adsorbent for removing bulky dye molecules from water. They proved that a mesoporous carbon with high surface area, large pore volume and bimodal pores showed the highest adsorption capacity among three selected OMCs with different pore structures. Recently, Yuan et al. (2013) adopted OMC as an adsorbent for the separation of CO<sub>2</sub> and N<sub>2</sub> from CH<sub>4</sub>, and the results indicated that OMC is a useful adsorbent, displaying both high selectivity and large adsorption capacity. These relevant studies indicate the superior adsorption properties of OMC. However, as a typical class of pollutant, the adsorption properties of VOCs on OMC have been relatively less studied, to the best of our knowledge.

In this study, OMC was synthesized via the EISA route and the adsorption properties of three typical kinds of VOCs on

OMC were studied to investigate the potential application of OMC in VOC adsorption. The selected VOCs were benzene, cyclohexane and hexane, which have different molecular structures based on six carbon atoms and are used in substantial amounts in industrial processes. The adsorption equilibrium and kinetics of the selected VOCs were studied and isosteric heats of adsorption were calculated. In addition, relationships between the adsorption properties and structures of the selected VOC molecule were discussed.

## 1. Materials and methods

### 1.1. Chemicals

Poly(propylene oxide)-b-poly(ethylene oxide)-b-poly(propylene oxide) triblock copolymer Pluronic F127 was purchased from Sigma-Aldrich Company. Ethyl silicate (SiO<sub>2</sub>, 28.4%+), phenol (99.5%+), formaldehyde solution (37.0%–40.0% aqueous solution), sodium hydroxide (96.0%), hydrochloric acid (36.0%–38.0%), ethanol (99.7%+), and hydrofluoric acid (40.0%+) were purchased from Sinopharm Chemical Reagent Company. All chemicals were used as received without any purification process. Deionized water was used in all the experiments.

### 1.2. Synthesis of materials

Resol was first prepared from phenol and formaldehyde solution in a base-catalyzed process and refrigerated for the later procedure. Then the OMC was synthesized via the EISA process with some minor modifications by our group (Gao et al., 2011). Typically, 1.6 g F127 was dissolved in 6.0 g ethanol at 313 K, then 5.0 g resol solution was added to form mixture A. 2.08 g TEOS was added into the 1.0 g HCl solution (0.2 mol/L) and stirred for 30 min at 313 K to form mixture B. Then, mixture B was poured into A. After stirring for 30 min, the solution was transferred into dishes. The transparent thin film was scraped from dishes after the evaporation of ethanol and placed into a tubular furnace for a further carbonization process. The film was calcined at 623 K for 3 hr under nitrogen protection with a heating rate of 2 K/min and a nitrogen flow of 50 mL/min, respectively. Then the temperature was raised to 1173 K with the heating rate being 1 K/min and remained 2 hr for further carbonization. After that, the obtained composite was stirred in HF solution for 12 hr to remove the silica and finally synthesized OMC was obtained after drying at 378 K for 5 hr.

### 1.3. Material characterization

X-ray diffraction (XRD) patterns were recorded on a PANalytical X'Pert PRO MPD using Cu-K $\alpha$  radiation ( $\lambda = 1.540598 \text{ \AA}$ ). High-resolution transmission electron microscopy (HRTEM) analysis was conducted on a JEOL 2011 microscope at 200 kV. Textural properties were obtained using nitrogen sorption isotherms at liquid nitrogen temperature on a NOVA 1200 gas sorption analyzer. The BET surface area was calculated using experimental points at relative pressures of  $P/P_0 = 0.05\text{--}0.25$ . Total pore volume was obtained by the nitrogen amount adsorbed at  $P/P_0 = 0.99$ . Pore size distributions were calculated by analyzing the desorption branch of isotherms based on the

Barrett-Joyner-Halenda (BJH) method. The thermogravimetric (TG) and differential thermogravimetric (DTG) analyses of samples were carried out on a Setaram Labsys-16 thermal analyzer. The heating rate was 10 K/min from 323 to 1173 K under an air flow of 30 mL/min.

#### 1.4. Static adsorption measurements

The adsorption properties of benzene, cyclohexane and hexane on OMC were measured on a Hidden Intelligent Gravimetric Analyzer IGA-002 (Hidden analytical company, Warrington, United Kingdom). The instrument is equipped with an electric heater that can be used to heat and blow out hot air to generate organic vapors. The OMC sample was located in a high vacuum chamber with a constant temperature with the adsorption temperature stabilized by a water bath. Before measuring, the relative pressures of the adsorption isotherms were set and recorded by computer. During the static adsorption procedure, organic vapors were controlled precisely by turbo molecular pump and allowed the adsorption to proceed following the set relative pressure values. In this work, 298, 308 and 318 K were selected as adsorption temperatures. The saturation vapor pressures of adsorbates were calculated following the Antoine equation (Speight, 2005):

$$\log p_0 = A - \frac{B}{T + C - 273} \quad (1)$$

where,  $p_0$  (Torr) is the saturated vapor pressure,  $T$  (K) is the temperature and  $A$ ,  $B$ , and  $C$  are the constants defined by the adsorbate; benzene (281–376 K):  $A = 6.90565$ ,  $B = 1211.033$ , and  $C = 220.790$ ; cyclohexane:  $A = 6.88617$ ,  $B = 1229.973$ , and  $C = 224.10$ ; and hexane (248–365 K):  $A = 6.87601$ ,  $B = 1171.17$ , and  $C = 224.41$ . The corresponding physico-chemical properties of the three kinds of VOCs are listed in Table 1 (Speight, 2005; Webster et al., 1998; Li et al., 2009).

## 2. Results and discussion

### 2.1. Characterization of OMC

The X-ray diffraction (XRD) patterns of the synthesized OMC are shown in Fig. S1 in the Supporting Information. The weak

broad diffraction peak around  $43^\circ$  in the wide-angle XRD pattern (a) indicates the long-range disorder of OMC. The well-defined diffraction peak at  $0.83^\circ$  in the small-angle XRD pattern (b) can be indexed as the (100) diffraction for a typical 2D hexagonal meso-structure, suggesting that the ordered mesoporous structure was formed successfully via the EISA method. The calculated cell parameter is 12.3 nm, according to the following equation:

$$a_0 = 2d_{100}/\sqrt{3}$$

where  $d_{100}$  is the (100) lattice spacing and can be calculated from the equation:

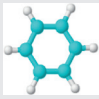
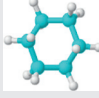
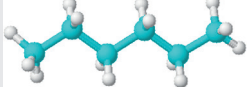
$$d_{100} = \lambda/2 \sin \theta.$$

In this study, the (100) lattice spacing is 10.6 nm. Fig. S2 shows the TEM image of the synthesized OMC taken from the direction perpendicular to the pore channels. The stripe-like arrangement of pores further confirms the 2D ordered meso-structure, although the XRD diffraction peaks in the range  $1\text{--}3^\circ$  were not as resolved as the diffraction peak at  $0.83^\circ$ .

Fig. S3 shows the TG analysis curve for OMC. The minor weight loss around 373 K was attributed to the loss of water and other small adsorbates. The main weight loss, approximately 100%, occurs between 573 and 973 K, suggesting that the silica component was almost completely removed by HF etching. Furthermore, the weight loss around 673 K is only 10% of the total weight, indicating that the synthesized OMC can be used under 673 K with a relatively high thermal stability.

Nitrogen adsorption/desorption isotherms and pore size distribution curve are depicted in Fig. S4. As shown in Fig. S4a, the isotherm can be divided into three parts. In the low relative pressure region ( $P/P_0 < 0.1$ ), small amounts of nitrogen were adsorbed onto OMC, indicating the existence of a small amount of micropores. As the relative pressure gradually raised, the adsorbed amounts of nitrogen increased and a typical adsorption/desorption hysteresis loop appeared. According to the definition of IUPAC, the type IV adsorption/desorption isotherm suggests the presence of mesopores (Sing, 1985). In addition, the corresponding H1 hysteresis loop at relative pressures between 0.5 and 0.8 suggests the

**Table 1 – Physical–chemical parameters of selected vapor adsorbate.**

Adsorbate	Structure	Relative molecular mass	Density (g/mL)	Boiling point/K	Molecular dimensions (Å)		
					x	y	z
Benzene		78.11	0.879	353	6.628	7.337	3.277
Cyclohexane		84.16	0.779	353.7	7.168	6.580	4.982
Hexane		86.18	0.660	342	10.344	4.536	4.014

existence of straight pore channels, in good agreement with the XRD data and the TEM image. In the high relative pressure region ( $P/P_0 > 0.8$ ), a plateau occurs in the isotherms and the adsorbed amounts of nitrogen stabilize at about  $1200 \text{ cm}^3/\text{g}$ . The calculated BET specific surface area and total pore volume are 1762 and  $1.75 \text{ cm}^3/\text{g}$  respectively, while the micropore volume is  $0.18 \text{ cm}^3/\text{g}$ . This value shows that most of the pore volume is from the mesopores rather than micropores. The BJH pore size distribution curve in Fig. S4b suggests that there is a bimodal-like pore size distribution, with the most probable pore sizes being 5.0 and 1.8 nm. The primary mesopore size corresponds to the main pore of the hexagonal channel originating from the removal of the triblock copolymer template, and the secondary mesopore comes from the etching of the silica component in the silica-carbon wall.

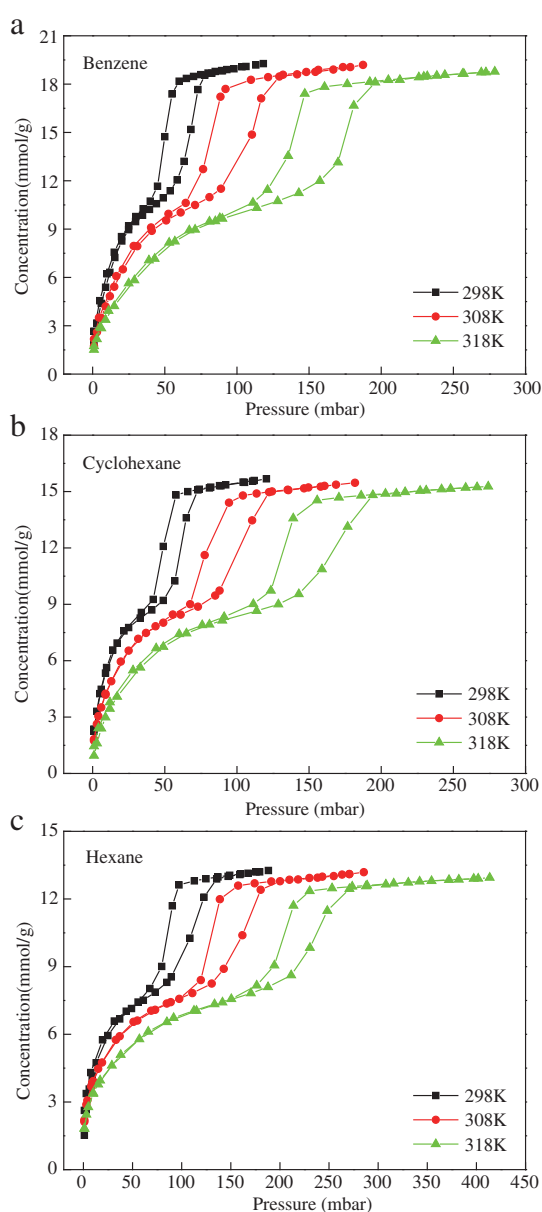


**Fig. 1 – Adsorption/desorption isotherms of benzene (a), cyclohexane (b), and hexane (c) onto ordered mesoporous carbon (OMC).**

**Table 2 – Adsorption amounts of selected vapor adsorbates under different temperature.**

Adsorbate temperature (K)		298	308	318
Benzene	Adsorption amount (mmol/g)	17.34	16.86	16.71
	Pore volume ( $\text{cm}^3$ )	1.54	1.50	1.49
Cyclohexane	Adsorption amount (mmol/g)	14.19	13.92	13.68
	Pore volume ( $\text{cm}^3$ )	1.53	1.51	1.48
Hexane	Adsorption amount (mmol/g)	11.97	11.85	11.82
	Pore volume ( $\text{cm}^3$ )	1.56	1.55	1.54

## 2.2. Adsorption of benzene, cyclohexane and hexane on OMC

Adsorption/desorption isotherms of benzene, cyclohexane and hexane onto OMC are depicted in Fig. 1. All adsorption isotherms show type IV isotherm behavior and exhibit three well-defined stages, just as in the nitrogen adsorption/desorption isotherm. At the initial stage, a sharp increase of adsorption occurs with the growth of saturated vapor pressure, suggesting high affinity between the three kinds of adsorbates and OMC. A similar increase in adsorption in the intermediate stage indicates multi-layer adsorption of adsorbates onto OMC. In addition, the hysteresis loops further confirm the mesoporous structure of OMC. In the final stage, with relatively higher vapor pressure, the adsorption of adsorbates reaches a saturation value, implying the available pore volume of OMC is completely filled. This corresponds to the finding in previous research that under high relative vapor pressure, the adsorbed amount is related to the available pore volume (Bell et al., 2011). The maximum adsorption amounts of each adsorbate were extrapolated based on the linear part of the third stage, and the corresponding amounts are depicted in Table 2. The adsorption of benzene reached 17.34 mmol/g at 298 K, and this value is higher than that obtained with other adsorbents (Yang et al., 2011; Yu et al., 2006; Wang et al., 2011; Fletcher et al., 2006). Furthermore, it is worthy to note that the amount adsorbed was about 7 mmol/g as the relative vapor pressure reached about  $P/P_0 = 0.1$ , showing a very useful property of OMC for the sorptive removal of VOCs at low concentrations (Jhung et al., 2007). For cyclohexane and hexane, the maximum adsorption amounts were 14.19 and 11.97 mmol/g respectively, lower than the corresponding benzene adsorption amount. In addition, the adsorption of each adsorbate gradually decreased with increasing temperature from 298 to 318 K, indicating the physical nature of the adsorption of VOCs on OMC. The pore volume of OMC available for VOC adsorption was also calculated using the adsorption amounts, and the liquid density of the adsorbates is shown in Table 1. As can be seen in Table 2, the pore volumes calculated for different adsorbates are similar, indicating that OMC is useful for the adsorption of both relatively small adsorbates like benzene and relatively larger adsorbates such as hexane, whose molecules behave as a plane and elongated cylinder, respectively. This universal adsorption property for both small and large adsorbates is important in circumstances where the exhaust gases include mixtures of VOCs such as benzene and hexane. This is

quite different from cases with some adsorbents that only selectively adsorb benzene over hexane, or where some adsorbates are excluded from a portion of the pores owing to the selective porosity of the adsorbents (Li et al., 2009; Reid and Thomas, 2001). Considering the textural properties of OMC, the universal adsorption properties may derive from the hierarchical pore size distribution of OMC. As revealed in Fig. S4, the OMC possesses a bimodal-like pore size distribution with the pore sizes of 5.0 and 1.8 nm, both of which are larger than the three dimensional sizes of the molecules studied, and thus fully accessible for benzene, cyclohexane and hexane.

### 2.3. Adsorption isotherms

Various adsorption isotherm equations are used to fit adsorption data. Among them, the virial equation is used extensively and the corresponding formula can be written in the form (Reid and Thomas, 2001),

$$\ln(n/p) = A_0 + A_1n + A_2n^2 + A_3n^3 \dots \quad (2)$$

where,  $n$  is the adsorbed amount at pressure  $p$ ;  $A_0$  is the first virial coefficient, which is related to the Henry's law constant  $K_0$  according to the equation  $K_0 = \exp(A_0)$ . The Henry's law constant  $K_0$  represents the interaction between the adsorbent surfaces and the adsorbed gas molecules. The second virial parameter ( $A_1$ ) is a function of adsorbate/adsorbate interactions.

In this research, the virial equation was adopted to simulate the adsorption isotherms of benzene, cyclohexane and hexane on OMC, and the corresponding virial parameters are listed in Table 3. It is clear that as the temperature increases, the  $A_0$  value is more negative, i.e. the  $K_0$  parameter decreases, suggesting a gradually weaker adsorbate–adsorbent interaction as the temperature increases from 298 to 318 K. This is in accordance with the exothermic characteristics of physical adsorption. Similarly, the  $A_1$  value becomes more negative, representing a weaker adsorbate–adsorbate interaction as the temperature increases. At the same temperature, the  $K_0$  value for the adsorbates varies in the order hexane > cyclohexane > benzene, reflecting the higher affinity of hexane than cyclohexane and benzene. This may be caused by the relatively higher molecular mass of hexane than the other two adsorbates, considering that adsorbates with higher molecular weight are more susceptible to adsorb on an adsorbent (Wang et al., 2012).

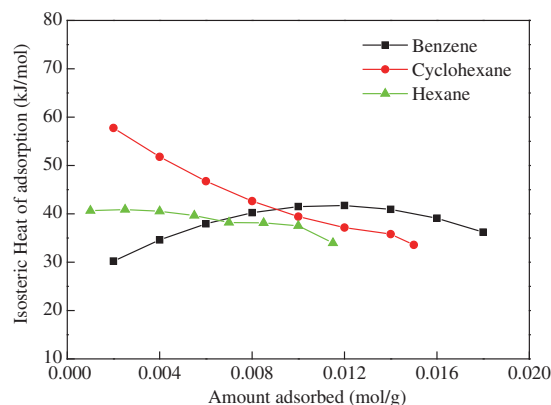


**Fig. 2 – Isosteric heats of adsorption for benzene, cyclohexane and hexane.**

### 2.4. Isosteric heats of adsorption

Isosteric heats of adsorption are important to evaluate the temperature change during the adsorption procedure. The value can be calculated from the isotherms measured at different temperatures using the Van't Hoff equation, which is given by the following expression,

$$\ln(p)_n = \frac{\Delta H_n}{RT} - \frac{\Delta S_n}{R} \quad (3)$$

where,  $\Delta H_n$  (kJ/mol) is the isosteric heat of adsorption,  $T$  (K) is adsorption temperature,  $p$  (Pa) is the pressure,  $R$  is the gas constant,  $n$  (mol/g) is the adsorbed amount, and  $\Delta S_n$  is the entropy of adsorption.

The values of the isosteric heats of adsorption for the three kinds of VOCs together with the amount adsorbed are depicted in Fig. 2. It can be observed that the isosteric heat of adsorption for cyclohexane and hexane gradually decrease as the amount adsorbed increases, suggesting that the properties of synthesized OMC are heterogeneous (Dou et al., 2011). The adsorption of benzene seems different from the other two adsorbates in that the isosteric heats of adsorption gently increase as the amount adsorbed increases. This may be related to the higher  $\pi$ – $\pi$  interaction between benzene molecules after multi-layer adsorption (Bell et al., 2011). As the adsorbed amounts increase, planar aromatic adsorbate

**Table 3 – Virial parameters for volatile organic compound (VOC) adsorption on OMC at 298 K, 308 K, 318 K.**

Adsorbate	Temperature (K)	$A_0$ (ln(mol/g/Pa))	$A_1$ (ln(g/mol))	$K_0$ ( $\times 10^{-6}$ )	$R^2$
Benzene	298	–11.210	–146.711	13.533	0.995
	308	–11.516	–177.493	9.972	0.983
	318	–11.813	–204.105	7.408	0.983
Cyclohexane	298	–10.554	–271.491	26.099	0.996
	308	–10.934	–304.584	17.836	0.986
	318	–11.649	–320.074	8.731	0.998
Hexane	298	–10.678	–385.938	23.040	0.999
	308	–10.803	–429.705	20.334	0.999
	318	–11.385	–413.608	11.361	0.999



molecules such as benzene are prone to stack with each other and structural rearrangement occurs, giving higher intermolecular  $\pi$ – $\pi$  interaction.

### 2.5. Adsorption kinetics

Adsorption kinetics are of fundamental importance to reveal the transport process of adsorbates into adsorbents. In our study, the mass relaxation data recorded by IGA can be used

to calculate the adsorption kinetics parameters. Several models such as linear driving force (LDF), double exponential and Fickian diffusion model have been used to describe the adsorption kinetics of gas adsorbates onto adsorbents (Bell et al., 2011). Previous studies have proved that the LDF model was followed for the adsorption of several kinds of gases/vapors on carbon adsorbents such as activated carbon and carbon molecular sieves (Fletcher et al., 2006; Reid and Thomas, 2001). In addition, the LDF model involves a simpler

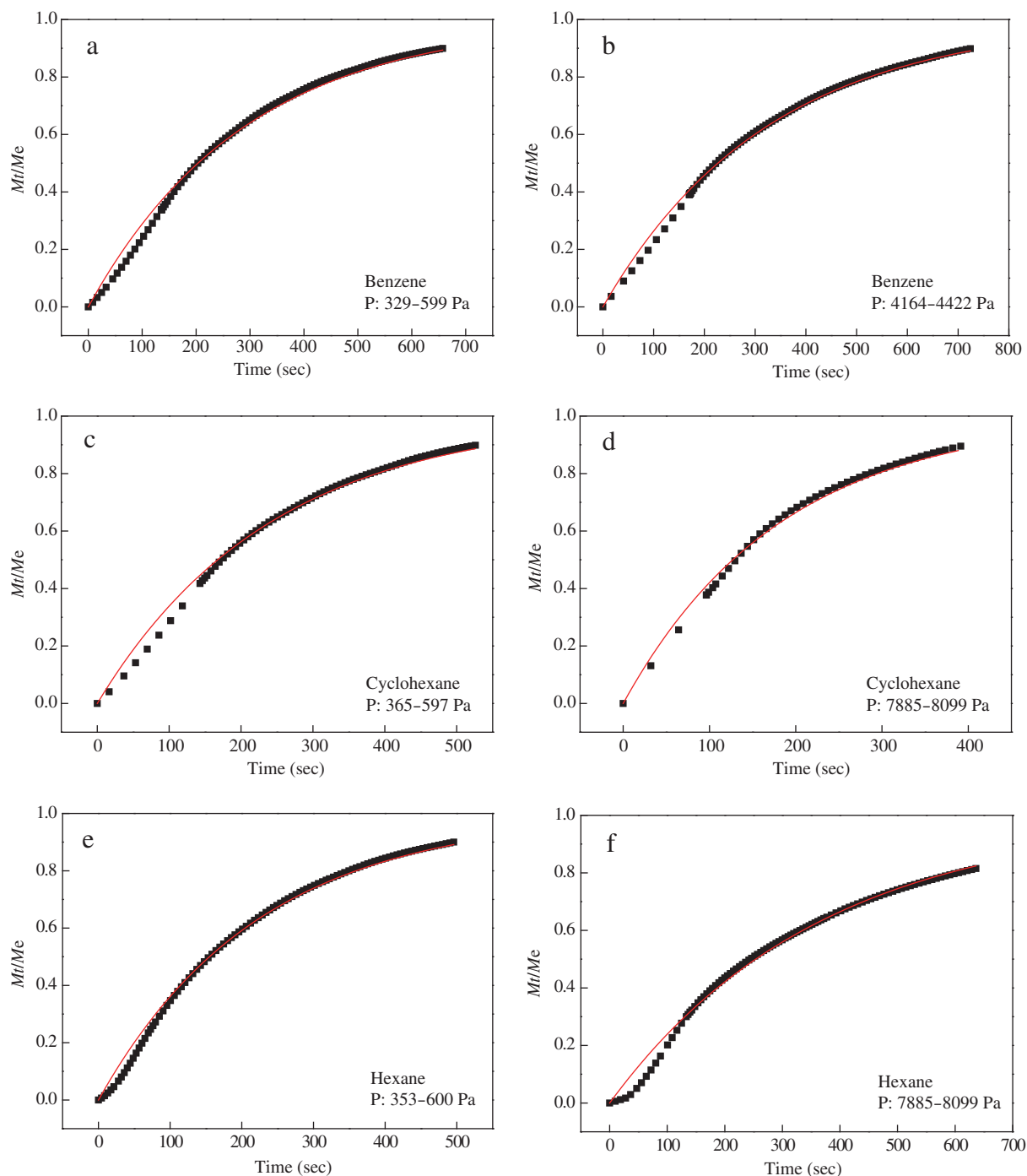


Fig. 3 – Adsorption kinetic profiles of benzene, cyclohexane, and hexane at 298 K on OMC, line is the linear driving force (LDF) model (every 20th points).

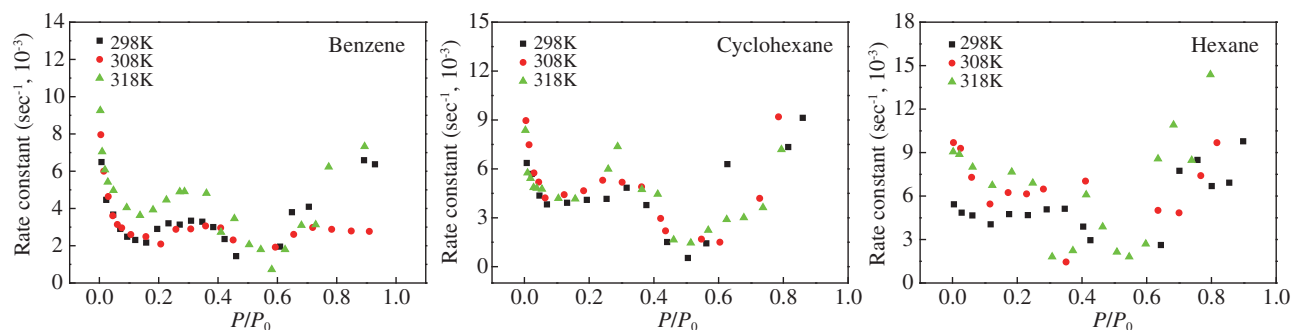


Fig. 4 – Kinetic rate constants of benzene, cyclohexane and hexane for adsorption on OMC with relative pressures under 298 K, 308 K, and 318 K.

expression compared with other models and can be described by the following equation,

$$M_t/M_e = 1 - e^{-kt} \quad (4)$$

where,  $M_t$  is the adsorbed amount at time  $t$ ;  $M_e$  is the equilibrium adsorbed amount for the given pressure increment, and  $k$  is the rate constant.

Typical adsorption kinetics data and the corresponding simulative LDF curves for benzene ( $P$ : 329–599 Pa, 4164–4422 Pa), cyclohexane ( $P$ : 365–597 Pa, 7885–8099 Pa) and hexane ( $P$ : 353–600 Pa, 8499–8950 Pa) at 298 K are depicted in Fig. 3. All graphs show that the adsorption kinetics obeys the LDF model with a good level of correlation. The slight deviation in the initial part of the simulated curves derives from the rapid changing of the vapor pressure in the instrument (Reid and Thomas, 2001). Further analysis verified that the adsorption kinetics of the three kinds of adsorbates at the experimental temperatures all follow the LDF model over most ranges of pressure.

The kinetic rate constants for the three kinds of adsorbates for each pressure step in the adsorption temperature range 298–318 K are shown in Fig. 4. For benzene adsorption at the selected temperature, the initial rate constant value at the lower relative pressure reaches about  $9 \times 10^{-3}$ , then a gradual decrease occurs with increasing relative pressure. The lowest rate constant appears when the relative pressures are between 0.4 and 0.6, in accordance with the value where capillary condensation occurs. This suggests a slower adsorption rate for the condensation step than the initial adsorption stage, which is similar to the adsorption rate of water vapor on carbon molecular sieves (O'koye et al., 1997). After the pore condensation process was completed, the rate constants increased to about  $8 \times 10^{-3}$ , which may be caused by the rearrangement of adsorbed benzene molecules, allowing increased accessibility into the pore structure (Foley et al., 1997). As can be seen in the figure, the change of adsorption rate constants for cyclohexane and hexane is similar to that for benzene, and the corresponding rate constants for cyclohexane and hexane in the initial relative pressure ranges are also about  $9 \times 10^{-3}$ . This indicates that the pore size of OMC is large enough and thus favorable for the diffusion of adsorbates with different molecular sizes. In contrast, as the pore size of a microporous adsorbent becomes narrower, adsorbates with larger sizes would cause a decrease in

the diffusion rate (Bell et al., 2011). Besides, it is notable that the kinetic rate constants at 318 K are larger than the corresponding values at 308 and 298 K for the three kinds of adsorbates, especially for benzene. This is reasonable if we consider the fact that a higher temperature will accelerate the diffusion of gas molecules. The diffusion properties of VOCs on other adsorbents such as activated carbon and carbon molecular sieves have been studied previously (Fletcher et al., 2006; Reid and Thomas, 2001). The corresponding results indicated that the diffusion rate constants of VOCs on activated carbon are mainly in the range of  $(2\text{--}4) \times 10^{-3}$ , which is almost half of the corresponding value for OMC. This suggests a relatively slower diffusion process for benzene in activated carbon than in OMC, as OMC possesses a larger pore size together with an ordered mesoporous structure.

It is generally accepted that the adsorption process of VOCs onto adsorbents can be described by the following steps: (1) mass transfer of adsorbates from the adsorbate phase to the surface of adsorbents, (2) diffusion of the adsorbate molecules into the pore channels of adsorbents, and (3) adsorption of adsorbates onto adsorbents (Wang et al., 2011). During our study, pure vapor of three kinds of adsorbates was generated and pumped to the adsorption chamber in which the adsorbents were located in a very short time, hence the mass transfer time of adsorbates can be neglected. Besides, the adsorption of adsorbates onto adsorbents is rapid compared with the other processes. Thus it is reasonable to assume that the adsorption process is controlled by the diffusion of adsorbate molecules into the pore channels of adsorbents. Previous studies pointed out that two kinds of barriers exist during the diffusion process: diffusion through the barrier at the pore entrance and diffusion along the pores (Fletcher et al., 2006; Reid and Thomas, 2001). The barrier around the pore entrance originates from the presence of discrete adsorption sites on the carbon basal plane of the outside surface. The adsorbate molecules must overcome the energy barrier to pass through the pore entrance and move into the inner part of the adsorbents. An LDF model is followed when the former barrier resistance is higher than the latter, i.e., the former process is the rate-determining step. In our research, the synthesized OMC has a bimodal-like pore size distribution with the pore sizes of 5.0 and 1.8 nm, respectively. Both sizes are much smaller than the molecular mean free path of the three kinds of organic vapors, which is important in evaluating diffusion properties, with a value usually more than 100 nm (Fletcher et al., 2006). Thus it is relatively difficult for the vapor

phase molecules to enter the pore channels of OMC. Furthermore, according to the principles of adsorption theory, a Knudsen diffusion process occurs when the mean free path of vapors is greater than the pore diameter and collisions between molecules of vapors are less frequent than collisions between vapor molecules and pore walls (Ruthven, 1984). Thus a general diffusion process of organic vapors onto OMC can be imagined such that the adsorption barrier originates from the difficulty VOC vapor molecules have in entering the pore channels of adsorbents and the following Knudsen diffusion, of which the former is the rate-determining step.

### 3. Conclusions

In this study, an OMC was synthesized via an EISA method and the resultant OMC has a large BET specific surface area and pore volume. Benzene, cyclohexane and hexane were selected as typical VOCs to evaluate the potential application of OMC as a VOCs adsorbent. The pore size of OMC is larger than and fully accessible to the adsorbates, thus the total pore volume can be used completely, and high adsorption amounts were achieved for all three VOCs in spite of their molecular size differences. Besides, the ordered mesoporous structure and the unusual bimodal-like pore size distribution, with the most probable pore sizes being 5.0 and 1.8 nm, enables the adsorbates to have a higher Knudsen diffusion rate in OMC compared with conventional adsorbents such as activated carbon and carbon molecular sieve. Therefore, the OMC might have great potential application in the VOC adsorption and recovery regime due to its superior adsorption capacity and faster diffusion process than microporous adsorbents.

### Acknowledgments

We gratefully acknowledge the financial support from the State Key program of National Natural Science Foundation (No. 21337003), the Strategic Priority Research Program (No. XDB05050200), the National High Technology Research and Development Program of China (2012AA063101), the Special Environmental Protection Foundation for Public Welfare Project (No. 201309073), and the Team Interaction and Cooperation of the Science and Technology Program of the Chinese Academy of Sciences.

### Appendix A. Supplementary data

Supplementary data to this article can be found online at <http://dx.doi.org/10.1016/j.jes.2014.10.015>.

### REFERENCES

Bell, J.G., Zhao, X., Uygun, Y., Thomas, K.M., 2011. Adsorption of chloroaromatic models for dioxins on porous carbons: the influence of adsorbate structure and surface functional groups on surface interactions and adsorption kinetics. *J. Phys. Chem. C* 115 (6), 2776–2789.

Britt, D., Tranchemontagne, D., Yaghi, O.M., 2008. Metal-organic frameworks with high capacity and selectivity for harmful gases. *Proc. Natl. Acad. Sci. U. S. A.* 105 (33), 11623–11627.

de Souza, S.M.D.G.U., da Luz, A.D., da Silva, A., de Souza, A.A.U., 2012. Removal of mono- and multicomponent BTX compounds from effluents using activated carbon from coconut shell as the adsorbent. *Ind. Eng. Chem. Res.* 51 (18), 6461–6469.

Dou, B., Li, J., Wang, Y., Wang, H., Ma, C., Hao, Z., 2011. Adsorption and desorption performance of benzene over hierarchically structured carbon-silica aerogel composites. *J. Hazard. Mater.* 196, 194–200.

Fletcher, A.J., Yüzak, Y., Thomas, K.M., 2006. Adsorption and desorption kinetics for hydrophilic and hydrophobic vapors on activated carbon. *Carbon* 44 (5), 989–1004.

Foley, N.J., Thomas, K.M., Forshaw, P.L., Stanton, D., Norman, P.R., 1997. Kinetics of water vapor adsorption on activated carbon. *Langmuir* 13 (7), 2083–2089.

Gao, W.J., Wan, Y., Dou, Y.Q., Zhao, D.Y., 2011. Synthesis of partially graphitic ordered mesoporous carbons with high surface areas. *Adv. Energy Mater.* 1 (1), 115–123.

Ghoshal, A.K., Manjare, S.D., 2002. Selection of appropriate adsorption technique for recovery of VOCs: an analysis. *J. Loss Prev. Process Ind.* 15 (6), 413–421.

Gonzalez-Miquel, M., Palomar, J., Rodriguez, F., 2013. Selection of ionic liquids for enhancing the gas solubility of volatile organic compounds. *J. Phys. Chem. B* 117 (1), 296–306.

Hartmann, M., Vinu, A., Chandrasekar, G., 2005. Adsorption of vitamin E on mesoporous carbon molecular sieves. *Chem. Mater.* 17 (4), 829–833.

He, C., Xu, L.L., Yue, L., Chen, Y.T., Chen, J.S., Hao, Z.P., 2012. Supported nanometric Pd hierarchical catalysts for efficient toluene removal: catalyst characterization and activity elucidation. *Ind. Eng. Chem. Res.* 51 (21), 7211–7222.

Hernandez, M.A., Velasco, J.A., Asomoza, M., Solis, S., Rojas, F., Lara, V.H., et al., 2003. Alkane adsorption on microporous SiO<sub>2</sub> substrata. 1. Textural characterization and equilibrium. *Energy Fuel* 17 (2), 262–270.

Jhung, S.H., Lee, J.H., Yoon, J.W., Serre, C., Ferey, G., Chang, J.S., 2007. Microwave synthesis of chromium terephthalate MIL-101 and its benzene sorption ability. *Adv. Mater.* 19 (1), 121–124.

Ji, L.L., Liu, F.L., Xu, Z.Y., Zheng, S.R., Zhu, D.Q., 2010. Adsorption of pharmaceutical antibiotics on template-synthesized ordered micro- and mesoporous carbons. *Environ. Sci. Technol.* 44 (8), 3116–3122.

Li, W., Zhao, D.Y., 2013. An overview of the synthesis of ordered mesoporous materials. *Chem. Commun.* 49 (10), 943–946.

Li, J.R., Kuppler, R.J., Zhou, H.C., 2009. Selective gas adsorption and separation in metal-organic frameworks. *Chem. Soc. Rev.* 38 (5), 1477–1504.

Lillo-Rodenas, M.A., Fletcher, A.J., Thomas, K.M., Cazorla-Amoros, D., Linares-Solano, A., 2006. Competitive adsorption of a benzene-toluene mixture on activated carbons at low concentration. *Carbon* 44 (8), 1455–1463.

Lin, H.W., Jang, M., Suslick, K.S., 2011. Preoxidation for colorimetric sensor array detection of VOCs. *J. Am. Chem. Soc.* 133 (42), 16786–16789.

Ma, T.Y., Liu, L., Yuan, Z.Y., 2013. Direct synthesis of ordered mesoporous carbons. *Chem. Soc. Rev.* 42 (9), 3977–4003.

Nevskaia, D.M., Castillejos-Lopez, E., Munoz, V., Guerrero-Ruiz, A., 2004. Adsorption of aromatic compounds from water by treated carbon materials. *Environ. Sci. Technol.* 38 (21), 5786–5796.

O'koye, I.P., Benham, M., Thomas, K.M., 1997. Adsorption of gases and vapors on carbon molecular sieves. *Langmuir* 13 (15), 4054–4059.

Parmar, G.R., Rao, N.N., 2009. Emerging control technologies for volatile organic compounds. *Crit. Rev. Environ. Sci. Technol.* 39 (1), 41–78.

Ramirez, D., Qi, S.Y., Rood, M.J., 2005. Equilibrium and heat of adsorption for organic vapors and activated carbons. *Environ. Sci. Technol.* 39 (15), 5864–5871.

- Reguer, A., Sochard, S., Hort, C., Platel, V., 2011. Measurement and modelling of adsorption equilibrium, adsorption kinetics and breakthrough curve of toluene at very low concentrations on to activated carbon. *Environ. Technol.* 32 (7), 757–766.
- Reid, C.R., Thomas, K.M., 2001. Adsorption kinetics and size exclusion properties of probe molecules for the selective porosity in a carbon molecular sieve used for air separation. *J. Phys. Chem. B* 105 (43), 10619–10629.
- Ruthven, D.M., 1984. *Principles of Adsorption and Adsorption Processes*. John Wiley-Interscience, New York, USA.
- Sing, K.S.W., 1985. Reporting physisorption data for gas/solid systems with special reference to the determination of surface area and porosity (Recommendations 1984). *Pure Appl. Chem.* 57 (4), 603–619.
- Speight, J.G., 2005. *Lange's Handbook of Chemistry*. 6th ed. McGraw-Hill, New York, USA.
- Tanaka, S., Doi, A., Matsui, T., Miyake, Y., 2013. Mass transport and electrolyte accessibility through hexagonally ordered channels of self-assembled mesoporous carbons. *J. Power Sources* 228, 24–31.
- Wang, S., Ang, H.M., Tade, M.O., 2007. Volatile organic compounds in indoor environment and photocatalytic oxidation: state of the art. *Environ. Int.* 33, 694–705.
- Wang, D., McLaughlin, E., Pfeffer, R., Lin, Y.S., 2011. Adsorption of organic compounds in vapor, liquid, and aqueous solution phases on hydrophobic aerogels. *Ind. Eng. Chem. Res.* 50 (21), 12177–12185.
- Wang, H., Jahandar Lashaki, M., Fayaz, M., Hashisho, Z., Philips, J.H., Anderson, J.E., et al., 2012. Adsorption and desorption of mixtures of organic vapors on beaded activated carbon. *Environ. Sci. Technol.* 46 (15), 8341–8350.
- Wang, S., Zhao, Q., Wei, H., Wang, J.Q., Cho, M., Cho, H.S., et al., 2013. Aggregation-free gold nanoparticles in ordered mesoporous carbons: toward highly active and stable heterogeneous catalysts. *J. Am. Chem. Soc.* 135 (32), 11849–11860.
- Webster, C.E., Drago, R.S., Zerner, M.C., 1998. Molecular dimensions for adsorptives. *J. Am. Chem. Soc.* 120 (22), 5509–5516.
- Wu, Y., Wang, R.J., Zhou, Y., Lin, B.H., Fu, L.X., He, K.B., et al., 2011. On-road vehicle emission control in Beijing: past, present, and future. *Environ. Sci. Technol.* 45 (1), 147–153.
- Yang, K., Sun, Q., Xue, F., Lin, D.H., 2011. Adsorption of volatile organic compounds by metal-organic frameworks MIL-101: influence of molecular size and shape. *J. Hazard. Mater.* 195, 124–131.
- Yu, M., Hunter, J.T., Falconer, J.L., Noble, R.D., 2006. Adsorption of benzene mixtures on silicalite-1 and NaX zeolites. *Microporous Mesoporous Mater.* 96 (1–3), 376–385.
- Yuan, B., Wu, X.F., Chen, Y.X., Huang, J.H., Luo, H.M., Deng, S.G., 2013. Adsorption of CO<sub>2</sub>, CH<sub>4</sub>, and N<sub>2</sub> on ordered mesoporous carbon: approach for greenhouse gases capture and biogas upgrading. *Environ. Sci. Technol.* 47 (10), 5474–5480.
- Zhuang, X., Wan, Y., Feng, C.M., Shen, Y., Zhao, D.Y., 2009. Highly efficient adsorption of bulky dye molecules in wastewater on ordered mesoporous carbons. *Chem. Mater.* 21 (4), 706–716.





## Editorial Board of Journal of Environmental Sciences

### Editor-in-Chief

**X. Chris Le** University of Alberta, Canada

### Associate Editors-in-Chief

**Jiuhui Qu** Research Center for Eco-Environmental Sciences, Chinese Academy of Sciences, China  
**Shu Tao** Peking University, China  
**Nigel Bell** Imperial College London, UK  
**Po-Keung Wong** The Chinese University of Hong Kong, Hong Kong, China

### Editorial Board

#### Aquatic environment

**Baoyu Gao** Shandong University, China  
**Maohong Fan** University of Wyoming, USA  
**Chihpin Huang** National Chiao Tung University, Taiwan, China  
**Ng Wun Jern** Nanyang Environment & Water Research Institute, Singapore  
**Clark C. K. Liu** University of Hawaii at Manoa, USA  
**Hokyoung Shon** University of Technology, Sydney, Australia  
**Zijian Wang** Research Center for Eco-Environmental Sciences, Chinese Academy of Sciences, China  
**Zhiwu Wang** The Ohio State University, USA  
**Yuxiang Wang** Queen's University, Canada  
**Min Yang** Research Center for Eco-Environmental Sciences, Chinese Academy of Sciences, China  
**Zhifeng Yang** Beijing Normal University, China  
**Han-Qing Yu** University of Science & Technology of China, China

#### Terrestrial environment

**Christopher Anderson** Massey University, New Zealand  
**Zucong Cai** Nanjing Normal University, China  
**Xinbin Feng** Institute of Geochemistry, Chinese Academy of Sciences, China  
**Hongqing Hu** Huazhong Agricultural University, China  
**Kin-Che Lam** The Chinese University of Hong Kong, Hong Kong, China  
**Erwin Klumpp** Research Centre Juelich, Agrosphere Institute, Germany

#### Peijun Li

Institute of Applied Ecology, Chinese Academy of Sciences, China  
**Michael Schloter** German Research Center for Environmental Health, Germany  
**Xuejun Wang** Peking University, China  
**Lizhong Zhu** Zhejiang University, China

#### Atmospheric environment

**Jianmin Chen** Fudan University, China  
**Abdelwahid Mellouki** Centre National de la Recherche Scientifique, France  
**Yujing Mu** Research Center for Eco-Environmental Sciences, Chinese Academy of Sciences, China  
**Min Shao** Peking University, China  
**James Jay Schauer** University of Wisconsin-Madison, USA  
**Yuesi Wang** Institute of Atmospheric Physics, Chinese Academy of Sciences, China  
**Xin Yang** University of Cambridge, UK

#### Environmental biology

**Yong Cai** Florida International University, USA  
**Henner Hollert** RWTH Aachen University, Germany  
**Jae-Seong Lee** Sungkyunkwan University, South Korea  
**Christopher Rensing** University of Copenhagen, Denmark  
**Bojan Sedmak** National Institute of Biology, Slovenia  
**Lirong Song** Institute of Hydrobiology, Chinese Academy of Sciences, China  
**Chunxia Wang** National Natural Science Foundation of China  
**Gehong Wei** Northwest A & F University, China

#### Daqiang Yin

Tongji University, China  
**Zhongtang Yu** The Ohio State University, USA

#### Environmental toxicology and health

**Jingwen Chen** Dalian University of Technology, China  
**Jianying Hu** Peking University, China  
**Guibin Jiang** Research Center for Eco-Environmental Sciences, Chinese Academy of Sciences, China  
**Sijin Liu** Research Center for Eco-Environmental Sciences, Chinese Academy of Sciences, China  
**Tsuyoshi Nakanishi** Gifu Pharmaceutical University, Japan

**Willie Peijnenburg** University of Leiden, The Netherlands  
**Bingsheng Zhou** Institute of Hydrobiology, Chinese Academy of Sciences, China

#### Environmental catalysis and materials

**Hong He** Research Center for Eco-Environmental Sciences, Chinese Academy of Sciences, China  
**Junhua Li** Tsinghua University, China  
**Wenfeng Shangguan** Shanghai Jiao Tong University, China  
**Ralph T. Yang** University of Michigan, USA

#### Environmental analysis and method

**Zongwei Cai** Hong Kong Baptist University, Hong Kong, China  
**Jiping Chen** Dalian Institute of Chemical Physics, Chinese Academy of Sciences, China  
**Minghui Zheng** Research Center for Eco-Environmental Sciences, Chinese Academy of Sciences, China  
**Municipal solid waste and green chemistry**  
**Pinjing He** Tongji University, China

### Editorial office staff

**Managing editor** Qingcai Feng  
**Editors** Zixuan Wang Suqin Liu Kuo Liu Zhengang Mao  
**English editor** Catherine Rice (USA)

# JOURNAL OF ENVIRONMENTAL SCIENCES

环境科学学报(英文版)

[www.jesc.ac.cn](http://www.jesc.ac.cn)

## Aims and scope

*Journal of Environmental Sciences* is an international academic journal supervised by Research Center for Eco-Environmental Sciences, Chinese Academy of Sciences. The journal publishes original, peer-reviewed innovative research and valuable findings in environmental sciences. The types of articles published are research article, critical review, rapid communications, and special issues.

The scope of the journal embraces the treatment processes for natural groundwater, municipal, agricultural and industrial water and wastewaters; physical and chemical methods for limitation of pollutants emission into the atmospheric environment; chemical and biological and phytoremediation of contaminated soil; fate and transport of pollutants in environments; toxicological effects of terrorist chemical release on the natural environment and human health; development of environmental catalysts and materials.

## For subscription to electronic edition

Elsevier is responsible for subscription of the journal. Please subscribe to the journal via <http://www.elsevier.com/locate/jes>.

## For subscription to print edition

China: Please contact the customer service, Science Press, 16 Donghuangchenggen North Street, Beijing 100717, China. Tel: +86-10-64017032; E-mail: [journal@mail.sciencep.com](mailto:journal@mail.sciencep.com), or the local post office throughout China (domestic postcode: 2-580).

Outside China: Please order the journal from the Elsevier Customer Service Department at the Regional Sales Office nearest you.

## Submission declaration

Submission of the work described has not been published previously (except in the form of an abstract or as part of a published lecture or academic thesis), that it is not under consideration for publication elsewhere. The publication should be approved by all authors and tacitly or explicitly by the responsible authorities where the work was carried out. If the manuscript accepted, it will not be published elsewhere in the same form, in English or in any other language, including electronically without the written consent of the copyright-holder.

## Editorial

Authors should submit manuscript online at <http://www.jesc.ac.cn>. In case of queries, please contact editorial office, Tel: +86-10-62920553, E-mail: [jesc@rcees.ac.cn](mailto:jesc@rcees.ac.cn). Instruction to authors is available at <http://www.jesc.ac.cn>.

## Journal of Environmental Sciences (Established in 1989) Volume 30 2015

<b>Supervised by</b>	Chinese Academy of Sciences	<b>Published by</b>	Science Press, Beijing, China
<b>Sponsored by</b>	Research Center for Eco-Environmental Sciences, Chinese Academy of Sciences		Elsevier Limited, The Netherlands
<b>Edited by</b>	Editorial Office of Journal of Environmental Sciences P. O. Box 2871, Beijing 100085, China Tel: 86-10-62920553; <a href="http://www.jesc.ac.cn">http://www.jesc.ac.cn</a> E-mail: <a href="mailto:jesc@rcees.ac.cn">jesc@rcees.ac.cn</a>	<b>Distributed by</b>	
		Domestic	Science Press, 16 Donghuangchenggen North Street, Beijing 100717, China Local Post Offices through China
		Foreign	Elsevier Limited <a href="http://www.elsevier.com/locate/jes">http://www.elsevier.com/locate/jes</a>
<b>Editor-in-chief</b>	X. Chris Le	<b>Printed by</b>	Beijing Beilin Printing House, 100083, China

CN 11-2629/X Domestic postcode: 2-580

Domestic price per issue RMB ¥ 110.00

ISSN 1001-0742

